Advanced in vitro models for studying drug induced toxicity

Ramaiahgari, S.C.

CHAPTER 2

A 3D *IN VITRO* MODEL OF DIFFERENTIATED HEPG2 CELL SPHEROIDS WITH IMPROVED LIVER-LIKE PROPERTIES FOR REPEATED DOSE HIGH-THROUGHPUT TOXICITY STUDIES

Sreenivasa C. Ramaiahgari[1], Michiel W. den Braver[2], Bram Herpers[1,4], Valeska Terpstra[3], Jan N.M. Commandeur[2], Bob van de Water[1] and Leo S. Price[1,4]

[1]Division of Toxicology, Leiden Academic Centre for Drug Research, Leiden University, Leiden, The Netherlands.

[2]Division of Molecular Toxicology, AIMMS, Vrije University Amsterdam, Amsterdam, The Netherlands.

[3]Department of Pathology, Bronovo hospital, The Hague, The Netherlands.

[4]OcellO B.V. Leiden, The Netherlands.

Archives of Toxicology 2014; 88(5): 1083-95

ABSTRACT

Immortalized hepatocyte cell lines show only a weak resemblance to primary hepatocytes in terms of gene expression and function, limiting their value in predicting drug induced liver injury. Furthermore, primary hepatocytes cultured on two-dimensional (2D) tissue culture plastic surface rapidly de-differentiate losing their hepatocyte functions and metabolic competence. We have developed a three-dimensional (3D) *in vitro* model using extracellular matrix-based hydrogel for long-term culture of the human hepatoma cell line HepG2. HepG2 cells cultured in this model stop proliferating, self organize and differentiate to form multiple polarized spheroids. These spheroids re-acquire lost hepatocyte functions such as storage of glycogen, transport of bile salts and the formation of structures resembling bile canaliculi. HepG2 spheroids also show increased expression of albumin, urea, xenobiotic transcription factors, phase I and II drug metabolism enzymes and transporters. Consistent with this, cytochrome P450–mediated metabolism is significantly higher in HepG2 spheroids compared to monolayer cultures. This highly differentiated phenotype can be maintained in 384 well microtiter plates for at least 28 days. Toxicity assessment studies with this model showed an increased sensitivity in identifying hepatotoxic compounds with repeated dosing regimens. This simple and robust high throughput-compatible methodology may have potential for use in toxicity screening assays and mechanistic studies and may represent an alternative to animal models for studying drug induced liver injury.

INTRODUCTION

Drug induced liver injury (DILI) has been a major cause of attrition during drug development [1]. The lack of accurate prediction with animal models and the increasing legislative pressure in implementing 3R's strategy demands an urgent need for robust *in vitro* models in safety assessment. *In vitro* human cell models offer many advantages compared to animal models. However, cells cultured *in vitro* on tissue culture plastic (2D), fail to develop normal tissue architecture, resulting in a poor level of differentiation and loss of tissue-specific functions, limiting their use as alternatives to animal models.

The liver is the principal site for drug metabolism. Liver parenchymal cells or hepatocytes contain the majority of the enzymes required for drug metabolism. Currently human primary hepatocytes are considered as the gold standard for drug metabolism and toxicity studies [2], but the limited availability of human liver samples, short life span, inter-donor differences and cost represent a significant limitation for *in vitro* screening assays [3]. With their unlimited life span, immortalized cell lines - in particular HepG2 cells - are commonly used as an alternative to primary cells [4]. However, in conventional 2D cultures, HepG2 cells express low levels of cytochrome P450 (CYP450) enzymes [5] and the xenobiotic receptors that regulate the expression of drug metabolic enzymes [6, 7]. Since the activity and inducibility of CYP450 enzymes is an important determinant of the pharmacokinetics and toxicity of drugs, poor expression of these and other metabolic enzymes in hepatocyte cell lines is thought to be a key factor in the poor prediction of toxicity in humans.

Hepatocytes are polarized epithelial cells with distinct apical and basolateral domains [8, 9]. The lateral domains of the adjacent hepatocytes form microvilli-lined bile canaliculi, which collect bile secreted from the hepatocytes [8]. This polarized morphology is lost when cells are restricted to hard plastic surface. Various 3D hepatocyte models have shown a significant improvement in maintaining the morphological and functional characteristics of liver tissue [10-15]. However, these models often require specialized equipment, are costly and/or not compatible with high volume screening. Here we describe a robust high throughput-compatible 3D *in vitro* model using HepG2 cells. HepG2 cells cultured in this model form polarized spheroids with functional bile canaliculi and strongly increased expression of albumin, genes encoding phase I and II drug metabolism enzymes, drug transporters and xenobiotic receptors that mediate induction of CYP450 enzymes. This highly differentiated phenotype can be maintained for more than 28 days in a microtiter plate allowing repeated or sub-chronic drug exposures. A 6-day repeated treatment on 3D HepG2 spheroids showed increased sensitivity in determining cytotoxicity of various hepatotoxic drugs compared to single acute exposures.

Therefore, this 3D HepG2 cell culture model represents a novel, relatively low cost method that is promising for routine high-throughput drug safety assessment containing many features reminiscent of metabolically competent human hepatocytes.

MATERIALS AND METHODS

Cell line

Human Hepatoma HepG2 cell line was obtained from American type tissue culture (ATCC, Wesel, Germany), cultured in Dulbecco's modified Eagles medium (DMEM) supplemented with 10% (v/v) fetal bovine serum (Invitrogen, Lot.no. 41F3161K), 25 U/mL penicillin, and 25 µg/mL streptomycin (PSA, Invitrogen).

3D cell culture

3D cell culture reagent, Matrigel (Cat.no: 354230; Lot: A6263, 24859, 2306532, 2104930), was obtained from BD Biosciences (Erembodegem, Belgium) and was used to culture liver spheroids. Batches of matrigel vary in the total protein concentration; a stock concentration of 5 mg/ml was prepared and used for culturing spheroids. A CyBi-Selma semi-automatic pipettor was used for liquid handling and dispensing. Cells were incubated at 37°C degrees with 5% CO2 and culture medium was refreshed every 2-3 days. 1000 cells (384 well plate) and 5000 cells (96 well plate) for 3D culture were used for optimal spheroid size. Samples for LC-MS Metabolite analysis, RNA extractions for qPCR, IHC analysis and toxicity assays were performed in 96-well plates. The remaining analyses were performed in 384 well plates.

Reagents and antibodies

Anti-human albumin (A80-229F, polyclonal), was from Bethyl laboratories Inc (Texas, USA), anti-β1-integrin antibody (MAB1981, monoclonal), was from Millipore (Amsterdam, Netherlands), anti-β-Catenin antibody (610153, monoclonal) and anti-Ezrin antibody (610602, monoclonal) was from BD transduction laboratories (Breda, Netherlands), anti-MRP2 (M2III-6) (AB3373, monoclonal) and anti-Ki-67 (AB15580, polyclonal) antibodies were obtained from Abcam (Cambridge, UK). Goat anti-mouse Alexa-488 (A11001) and anti-rabbit Alexa-488 (A11008) were from Molecular Probes (Breda, Netherlands). Hoechst 33258 from Sigma (Zwijndrecht, Netherlands) (2 µg/ml) was used to visualize the nuclei of fixed cells and Hoechst 33342 (200 ng/mL) from Fisher Scientific (Leiden, The Netherlands) for live cells. Rhodamine phalloidin was obtained from Sigma (Zwijndrecht, Netherlands).

Albumin and urea measurements

Albumin in cell culture supernatant was measured using human albumin ELISA kit from abcam (ab108788) according to the manufacturer's protocol. Samples were

collected after 72 hours of initial cell seeding from 2D cultures. Changing the culture media every 2-3 days was essential for optimal spheroid growth in 3D cultures and so a 72-hour cumulative albumin secretion was measured at day 3, 7, 14, 21 and 28. Cell number was estimated at each time point using ATPlite reagent (PerkinElmer) and the data normalized to 6x104 cells. Urea was measured using a colorimetric assay kit from BioVision (California, USA). Cultures were briefly washed with PBS and homogenized with urea assay buffer and analyzed according to manufacturers protocol.

Histological and immunohistochemical analysis

HepG2 cell spheroid suspension was collected in PBS and spun at 1000 rpm for 5 minutes. The pellet was fixed in 10% buffered formalin and embedded in paraffin. 3 μm tissue sections were prepared and stained with haematoxylin and eosin, PAS (Periodic acid-Schiff's reaction) and PAS after treatment with diastase to remove glycogen. Human liver tissue was provided by Bronovo Hospital, The Netherlands, in accordance with the hospital's code of conduct regarding use of patient-derived material. Immunohistochemical detection of cytokeratin 7 and 8 (CAM5.2, 1:20, BD Biosciences, Ref. 345779) and bile canaliculi (polyclonal CEA, 1:200, DAKO, Ref. A0115) was performed using an automated immunostainer (Benchmark ULTRA, Roche Diagnostics).

RNA extraction and Real time PCR analysis

Total RNA was extracted using Trizol reagent (Invitrogen) followed by clean up with RNeasy mini kit (Qiagen). 500 ng of RNA was used for cDNA synthesis using Revert aid First strand cDNA synthesis kit (Thermo Scientific) according to the manufacturer's instructions. Real time PCR was performed using SYBR green master mix (Applied Biosystems). mRNA levels of target genes were normalized to housekeeping gene, GAPDH. The list of primer sequences is shown in supplementary table S3.

Determination of CYP450 enzyme metabolic activity

2D and 3D cultures were incubated with a mixture of probe substrates, including: diclofenac (CYP2C9, 50 µM), midazolam (CYP3A4, 10 µM), bufuralol (CYP2D6, 20 µM) and chlorzoxazone (CYP2E1, 100 µM). Cell culture supernatants were collected at 0-, 4-, 24- and 48-h post exposure and stored at -80 degrees. LC-MS analysis of metabolites was performed at Pharmacelsus GmbH (Saarbrucken, Germany). Detailed methodology used is described in supplementary data S4. Diclofenac and chlorzoxazone were obtained from Sigma-Aldrich (Zwijndrecht, Netherlands). Bufuralol HCL was from Corning Gentest (Amsterdam, Netherlands), midazolam was from Actavis (Hafnarfirdi, Iceland).

Determination of glucuronidation and sulfation activity

2D and 3D cells were incubated with 500 µM diclofenac and 1 mM acetaminophen to study glucuronidation and sulfation activity. A detailed protocol is in the supplementary data S6.

Analysis of hepatobiliary transport in HepG2 cells

Cholyl-lysyl-fluorescein, CLF (BD Biosciences) a synthetic fluorescent bile acid analogue with similar biological activity as cholyl glycine was used to determine the hepatobiliary transport activity. 2D and 3D HepG2 cells were rinsed with 1x Hanks balanced salt solution (Invitrogen, Breda, Netherlands) and incubated with 2 µM CLF in HBSS for 45 minutes similar to the protocol used for primary rat hepatocytes [16]. After the incubation period the cells were washed 3 times with HBSS and imaged live by confocal microscopy (Nikon TiE2000, Nikon). A series of images were collected across the Z-plane of the spheroid and a maximum intensity projection image was generated using the image processing software package, Image J.

Assessment of drug-induced toxicity

2D and 3D HepG2 cells were cultured for 24 hours and 21 days respectively prior to compound exposure. Bosentan was obtained from Sequoia Research Products (Pangbourne, UK), all the other compounds were obtained from Sigma-Aldrich (Zwijndrecht, Netherlands). The concentrations of the compounds and solvents used are as shown in the supplementary data S7. A maximum concentration of up to 100X Cmax or above was tested (a reference scaling factor as used in earlier studies with primary hepatocytes [17, 18]). Compounds that are not toxic at 100X Cmax and that are soluble in culture media were tested up to 100 mM (acetaminophen, isoniazid and valproic acid). Cell death was estimated as percentage of viable cells after compound exposure compared to its vehicle control. ATP-lite luminescence assay kit (PerkinElmer) was used to measure cell viability. Measurements were recorded 24-hours after drug exposure. Additionally a repeated drug exposure was performed on 3D cell cultures, by adding the compound every 24 hours for 6 days (at day 22, 23, 24, 25, 26, 27 of spheroid culture) and measuring cell viability on 7th day (day 28 of spheroid culture).

Statistical analysis

Data expressed is either representative of 3 independent experiments (mean ± standard deviation (± S.D.) or mean of 3 independent experiments (± S.D.). Graphs were plotted using Graphpad Prism 4 (Graphpad software, San Diego, CA, USA).

RESULTS

HepG2 cell proliferation and differentiation in 3D cultures

5000 or 1000 cells in suspension were added on top of a pre-cast gel in 96 or 384-well microplates, respectively. Maintaining this cell number was critical for optimal spheroid size (~100 µm). After seeding, cells settled, adhered to the gel and self-aggregate to form cell clusters (87+/- 16 clusters per well in a 384 microplate) (Supplementary Figure S1). These gradually formed well-defined spheroids over a period of 21 days. The average diameter of the spheroids at day 28 was 118 ± 5 µm (supplem-entary Figure S1), which is sufficient for oxygen diffusion, as spheroids above 200 µm are known to become hypoxic at the core [19] [20]. To examine the effect of 3D culture on cell proliferation, HepG2 cells were immunostained with antibodies against the proliferation marker Ki-67. The majority of HepG2 cells in 2D

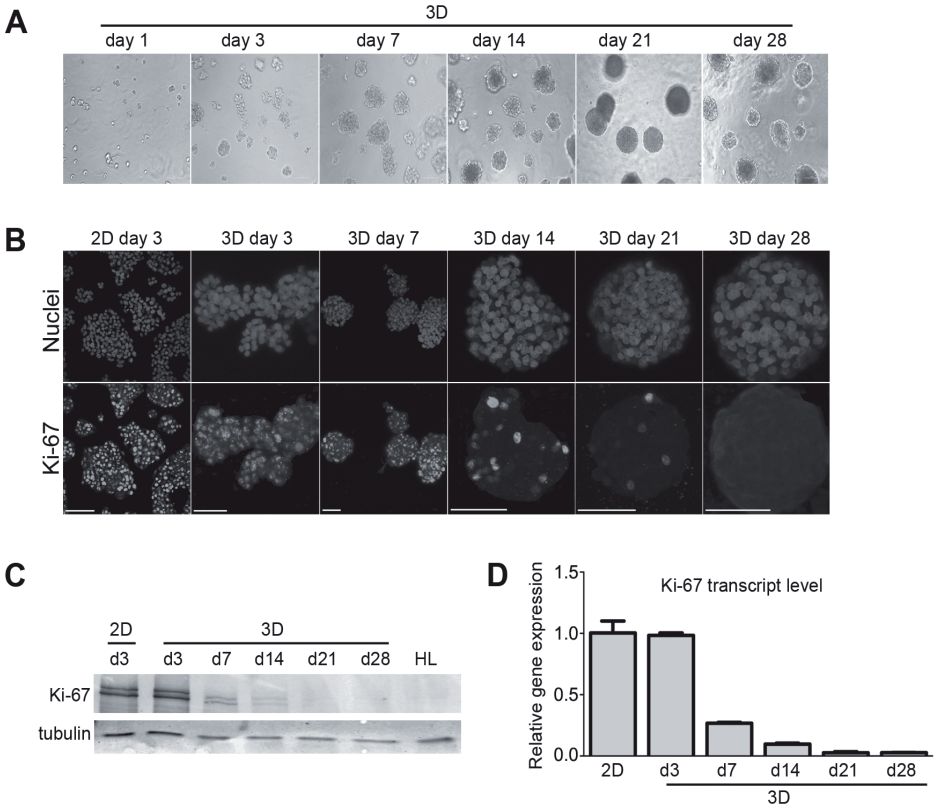

Figure 1. *Spheroid development in 3D culture*. Phase contrast images of HepG2 cells cultured in Matrigel (A) scale bar 100 µm. Immunostaining of HepG2 cells for the proliferation marker, Ki-67, counterstained with Hoechst 33358 for nuclei (Blue) (B). Scale bar – 50 µm. Ki-67 protein level assessed by Western blot analysis; HL= Human Liver (C) and Real time PCR transcript analysis (D), Data is representative of 3 independent experiments.

culture were positive for Ki-67 (Fig. 1B). However, in 3D cultures, there was a sharp decline in Ki-67 positive cells between day 7 and 14, and positive cells were barely present after 21 days. This was confirmed by analyzing the protein and mRNA transcript levels of Ki-67 (Fig. 1C and D). Together, these data demonstrate that HepG2 cells transform from a highly proliferative state in monolayer culture to non-proliferating spheroids after a period in 3D culture.

HepG2 cells form functionally differentiated spheroids in 3D culture

Primary hepatocytes cultured as monolayers lose tissue-specific polarity and function and eventually die [21]. Differentiated HepG2 spheroids acquire a uniform size, which remains stable after 21 days. Larger spheroids can show signs of necrosis in the center due to hypoxia [20]. H&E staining of HepG2 spheroids show organized nuclei and cytoplasm and did not show signs of necrosis although the formation of large and multiple cavities was occasionally observed (Fig. 2B). Since the proliferation of HepG2 cells in 3D culture ceased, we anticipated a probable reprogramming into a more differentiated liver cell phenotype. Positive immunostaining for cytokeratins 7 and 8 at cell-cell junctions in HepG2 spheroids indicate that the cells of the spheroid retain epithelial characteristics (Fig. 2B). To further study the differentiation of the cells in the spheroid we examined the expression of apico-basal surface epithelial markers by immunofluorescent staining. An intense staining of the basal membrane marker, β1 integrin, was seen at the margins of the spheroid where cells contact the extracellular matrix. β-catenin, which is associated with E-cadherin at sites of cell-cell contacts, was localized at lateral junctions. Together, the localization of these two markers indicates that the cells at the periphery of the spheroid establish basal-lateral polarity (Fig. 2A). Finally, we determined the formation of bile canaliculi-like structures by examining the localization of the canalicular marker glycoprotein-1 [22]. HepG2 spheroids showed enhanced punctate staining for this marker between some cells with a similar pattern of immunohistochemical staining to that of human liver (Fig. 2B). We substantiated this with additional immunofluorescent stainings for MRP2 and ezrin (Fig. 2A) that are typically associated in actin rich regions of the bile canaliculi [23, 24]. The localization of these markers was also observed in distinct punctae, which are suggestive of rudimentary canaliculi.

We also investigated the metabolic differentiation by evaluating the glycogen storage capacity, a typical function of liver hepatocytes. 3D spheroids showed the presence of intracellular glycogen as determined by periodic acid-Schiff (PAS) staining. As a control, spheroids were also treated with diastase to digest the glycogen, which resulted in decreased intracellular PAS staining confirming the presence of glycogen in 3D HepG2 spheroids (Fig. 2B).

Cell polarity and ECM signaling have been shown to promote liver-specific

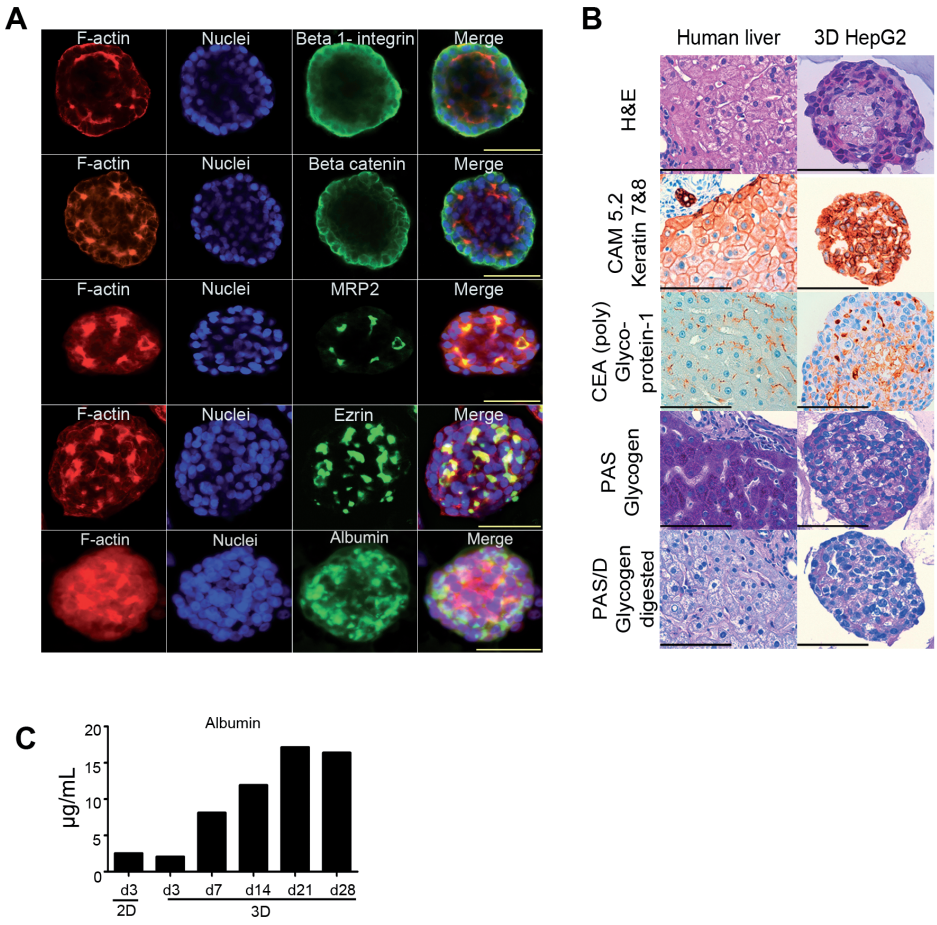

Figure 2. *3D HepG2 spheroids show increased expression of markers of differentiated and polarized hepatocytes*. Immunofluorescence staining of 3D HepG2 spheroids with epithelial cell markers β1-integrin, β-catenin, MRP2, ezrin and albumin counterstained with Rhodamine-phalloidin for F-actin and Hoechst 33358 for nuclei (A), scale bars - 50 µm. Histological examination of human liver and HepG2 spheroids (B) scale bars - 100 µm. Albumin production in 2D and 3D HepG2 cells in 72 hours (C) data normalized to 6X104 cells (n=2).

functions such as albumin secretion and metabolic enzyme expression [25]. Immunostaining of HepG2 spheroids showed the presence of albumin (Fig 2A). Consistently, mRNA expression levels of albumin were 10± 4 fold higher in differentiated 3D HepG2 cultures compared to 2D cultures (Fig. 3B). Albumin protein level was approximately 16 µg/mL at day 21 and day 28 (Fig. 2C). Urea production was also found to be higher in spheroids (Supplementary S2). Taken together, these data suggest that HepG2 cells undergo structural and metabolic differentiation in 3D ECM hydrogels.

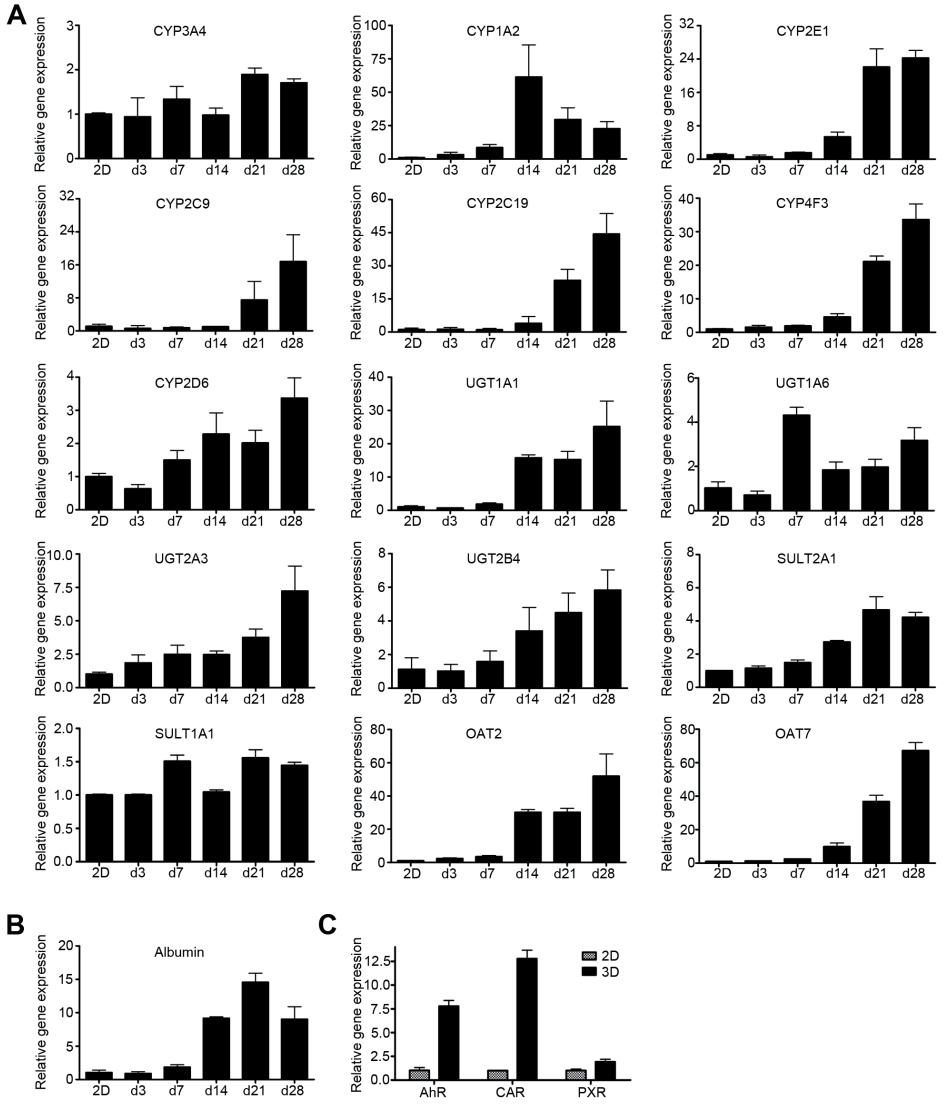

Figure 3. *Real-time PCR analysis of liver-specific markers and metabolic enzymes in 2D and 3D culture.* Fold-change gene expression levels of 3D spheroids at day 3 (d3), day 7 (d7), day 14 (d14), day 21 (d21) and day 28 (d28) compared to 3-day cultured 2D HepG2 cells (2D) (A). Data are representative of 4 individual experiments. Real time PCR analysis of Albumin (B); and nuclear receptors AhR, CAR and PXR in 3D cell cultures (C) compared to 2D cultures. Data normalized to GAPDH, representative of 3 independent experiments.

Metabolic competence is enhanced in 3D-cultured HepG2 spheroids

Low levels of drug metabolism enzymes in HepG2 cells contribute to mis-classification of chemical entities that form toxic metabolites [5]. Real time PCR analysis showed higher expression of various phase I and II metabolizing enzymes and drug

transporters in 3D HepG2 spheroids compared to 2D cultures (Fig. 3A). mRNA transcript levels of phase I xenobiotic metabolic enzymes CYP3A4, CYP1A2, CYP2E1, CYP2C9, CYP2C19, CYP4F3 and CYP2D6 were systematically analyzed over a period of 28 days of spheroid development. Expression levels increased, with a tendency to stabilize after day 14, which coincided with reduced cell proliferation and expression of differentiation markers (Fig. 2). Similarly, the mRNA levels of several phase II xenobiotic metabolizing enzymes UGT1A1, UGT1A6, UGT1A3, UGT2B4, SULT2A1 also increased during 3D culture. Phase III enzyme drug transporters also play a major role in the formation of metabolites and in drug detoxification. The expression levels of OAT2 and OAT7, which represent major transporters of various clinically relevant drug classes [26, 27], were highly increased in spheroids compared to 2D culture.

To evaluate whether increased mRNA levels of metabolic enzymes correlated with an increased functional metabolism, we compared the ability of 2D and 3D cultured HepG2 cells to metabolize CYP450 specific substrates. Rate of formation of 4'-hydroxydiclofenac catalyzed by CYP2C9 was profoundly higher in 3D spheroid cultures and this metabolite was not seen in 2D cultured HepG2 cells (Fig. 4). Day 21 and day 28 spheroid cultures had similar metabolic activity which further substantiates a stable differentiated phenotype after 21-days in 3D culture. Similarly, 1'-hydroxymidazolam, a metabolite of the major CYP450 enzyme, CYP3A4, was approximately 15, 30 and 40 nM at T= 4, 24 and 48, whereas in 2D cells the metabolite reached a maximum of 6 nM at 48 hours. 1'-hydroxybufuralol, a metabolite of bufuralol mediated by CYP2D6, was significantly higher in 3D spheroid cultures (10 nM (4h), 30 nM (24h) and 60 nM (48h) respectively), compared to 2D cultures (3 nM (4h), 10 nM (24h) and 20 nM (48h)). 6'-hydroxychlorzoxazone formation, which is mediated by CYP2E1, was seen in 2D HepG2 cultures but no profound metabolism was observed in 3D spheroids for the concentration used (Fig 4). This was unexpected, since CYP2E1 mRNA was approximately 20-fold higher in 3D compared to 2D cultures. Further investigation is required to determine whether the metabolite is not generated or whether the compound has an affinity to bind to the hydrogel in our 3D model.

Additionally, phase I enzyme activity was assessed by studying the metabolism of testosterone. Testosterone undergoes oxidative metabolism by various CYP450 enzymes, forming several metabolites [28]. The formation of metabolites increased in HepG2 spheroids compared to 2D culture. These include a major metabolite, androstenedione (Supplementary S5) consistent with previous observations [29]. In addition, a small quantity of 6β-hydroxy-testosterone was observed which was significantly increased in spheroids and 1β-hydroxy-testosterone which was detected only in 3D cell cultures but below the detection threshold level in 2D HepG2

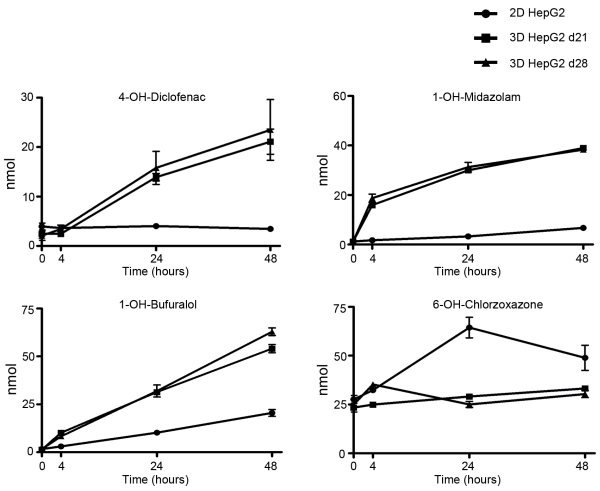

Figure 4. *Comparison of Phase I enzyme activity in 2D and 3D culture.* CYP450 enzyme activity as measured by rate of formation of OH-diclofenac (CYP2C9), OH-midazolam (CYP3A4), OH-bufuralol (CYP2D6), OH-chlorzoxazone (CYP2E1). Data is represented as mean of three independent experiments ± SD; (n=3), minimum detection level for Diclofenac is 2 nM and Chlorzoxazone is 25 nM.

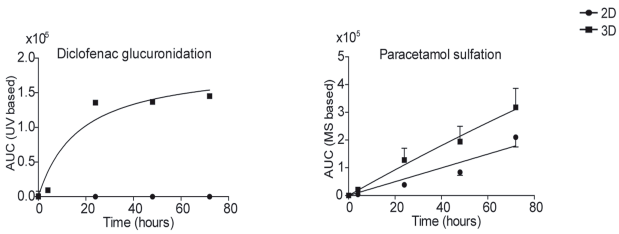

Figure 5. *Comparison of Phase II enzyme activity in 2D and 3D culture*. Rate of formation of acyl glucuronides from diclofenac and sulfation activity of acetaminophen in 2D HepG2 cells and 3D day 28 spheroid cultures. Data is representative of two independent experiments.

cell cultures (Supplementary S5 D&E). An unidentified hydroxy-metabolite was also observed only in 3D HepG2 cell cultures, although the level was too low for detailed quantification (data not shown).

Phase II metabolism was investigated using diclofenac (glucuronidation) and acetaminophen (sulfation) as probe substrates. The rate of diclofenac glucuronidation was significantly upregulated in 3D HepG2 cultures. The data shown in Fig. 5 was based on the sum of four different acyl glucuronides as described previously [30]. In contrast, there was only a limited difference in acetaminophen sulfation between 2D and 3D cultures (Fig. 5), which was consistent with the expression level of of SULT1A1 mRNA (Fig. 3A), which is involved in sulfation of acetaminophen. The same trends for phase II metabolism (glucuronidation and sulfation) were obtained when 7-hydroxy coumarin was used as substrate (data not shown).

Together, these data indicate that the differentiation of HepG2 cell spheroids is associated with an increased expression of numerous phase I, II and III enzymes

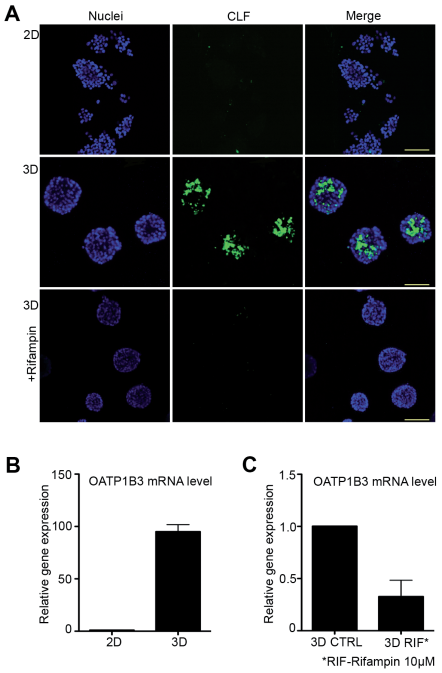

Figure 6. *Functional analysis of bile acid transport in 3D HepG2 spheroids*. Cholyl-lysyl-fluorescein (CLF) accumulation in 2D and 3D HepG2 cells (A) scale bars - 100 μm. mRNA transcript level of OATP1B3 in 3D compared to 2D culture (B). mRNA transcript level of OATP1B3 in 3D cell cultures after rifampin treatment (C); data normalized to GAPDH, representative of three independent experiments.

that critically determine ADME of xenobiotics. This functionally correlates with an increased xenobiotic metabolic competence.

Basal level expression of xenobiotic nuclear receptors in HepG2 cells

Various compounds induce ADME related genes by receptor-mediated mechanisms, resulting in drug-drug interactions that affect the pharmacokinetic and pharmacodynamic properties of a second administered drug [31]. We therefore examined the basal expression level of nuclear receptors AhR, CAR and PXR by real time PCR. These were found to be expressed 7.7-, 12.7-, and 1.9- fold higher respectively in HepG2 spheroids compared to 2D HepG2 cultures (Fig. 3C), suggesting that our spheroid system may be more responsive to the inducers of these receptors.

Functional bile canaliculi are formed in HepG2 spheroids

Bile salts are transported by hepatocytes into the bile canaliculi. Perturbation of this process is often associated with drug-induced liver injury. To evaluate bile transport, we used a synthetic bile acid analogue, cholyl-lysyl-fluorescein (CLF). CLF accumulated in canaliculi structures of 3D HepG2 spheroids, suggesting that these indeed represent rudimentary canaliculi (Fig. 6A). In contrast, there was no detectable accumulation of CLF in 2D HepG2 cultures. Uptake of CLF into hepatocytes in human liver is mediated by transporter OATP1B3 [32] and excreted into canaliculi via transporters including MRP2 [32]. Immuno-staining of MRP2 on HepG2 spheroids clearly

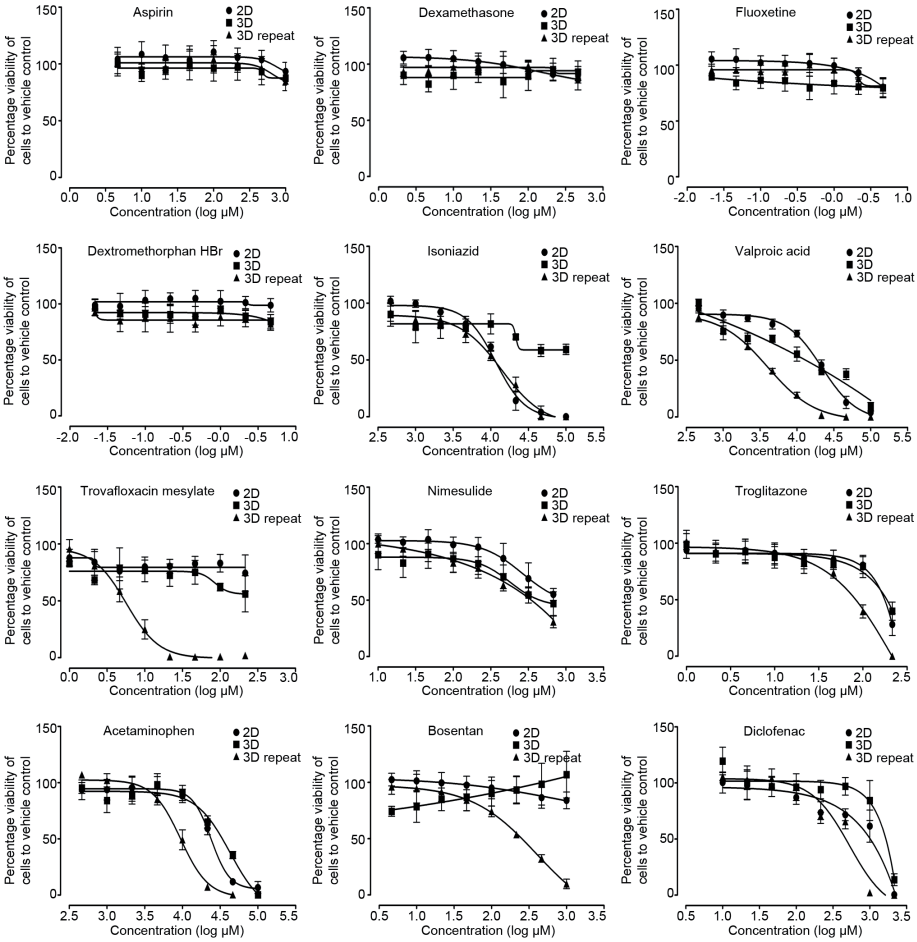

Figure 7. *Drug induced cytotoxicity in 2D and 3D HepG2 cells.* ATP content of 2D HepG2 (*filled circle*), 3D HepG2 (*filled square*) after 24 hour drug exposure and 3D HepG2 6-day repeated drug exposure (*filled triangle*) to non-hepatotoxic compounds, ATP-lite assay was performed to measure the cell viability and assess cytotoxicity. Data is mean of 3 independent experiments (±SD).

shows its presence in the apical regions (Fig. 2A). The mRNA level of OATP1B3 was found to be 95–fold higher in HepG2 spheroids compared HepG2 monolayer cultures (Fig. 6B). Inhibition of OATP1B3 with rifampin [25, 33] inhibited the transport of CLF into the bile canalicular regions (Fig. 6A). Consistent with this, mRNA level of OATP1B3 was also significantly downregulated after 24-hour treatment with rifampin (Fig. 6C). These results suggest that HepG2 spheroids are able to take up bile salts and actively transport them into canalicular structures via known drug transporters.

Assessment of drug-induced toxicity

In addition to impaired drug metabolism, the scope for chronic drug exposure is restricted in monolayer cultures due to the high rate of proliferation. We evaluated whether our HepG2 spheroid model could overcome these limitations by determining the cytotoxicity of several hepatotoxicants that require bio-activation and typically demonstrate liver injury after repeated dosing. Four compounds that were non-hepatotoxic in previous studies (aspirin, dexamethasone, fluoxetine and dextromethorphan) [17, 18] were similarly not toxic in 2D and 3D HepG2 cell cultures. In contrast, sensitivity to most hepatotoxic compounds was considerably increased with repeated drug exposures in 3D spheroids (Fig. 7). The TC50 of trovafloxacin mesylate, a drug withdrawn from the market, was near to the peak human plasma concentration (Cmax = 4.078 μM; TC50 after repeated dose in 3D is 5.6 μM), whereas in 2D, this compound was not toxic up to 100X Cmax. For most other hepatotoxic compounds, the TC50 was less than or close to 100X Cmax (see supplementary table S7). In conclusion, our 3D spheroid system can report cytotoxicity of known hepatotoxicants, where 2D HepG2 model systems often fail.

DISCUSSION

One of the major drawbacks with current drug safety evaluation studies is the failure of *in vitro* test models to adequately reflect hepatotoxic responses in humans. Here we present an ECM hydrogel–based 3D cell culture model using HepG2 cells for hepatotoxic studies. This system involves the re-programming of otherwise dedifferentiated HepG2 cells to acquire critical lost functions of *in vivo* hepatocytes including formation of bile canaliculi-like structures, bile acid transport, improved drug metabolism, transporter activity and sensitivity to hepatotoxicants. The compatibility with standard assay plates and automation equipment makes this approach suitable for high-throughput toxicity screening.

HepG2 spheroids in this model differentiate and show many phenotypic characteristics of hepatocytes *in vivo*, such as reduced proliferation, localization of apical and basal-lateral markers and markers for canaliculi. Reduced proliferation may be a result of contact inhibition of growth driven by increased cell-cell interactions. Formation of bile canaliculi was reported earlier in sandwich cultured human and primary rat hepatocytes cultures [21, 34, 35]. Bile-canalicular structures were also observed in hanging drop cultures of HepG2 cells [36, 37]. Recently a 3D peptide nanofiber matrix was also shown to induce a spheroid phenotype and bile canaliculi formation with HepG2 cells, although these spheroids comprised fewer cells and did not result in up-regulation of metabolizing enzymes [38]. In contrast, we found that micro-environmental cues drive both structural organization of canaliculi and the expression and function of drug metabolizing enzymes and transporters.

The accumulation of the CLF in HepG2 spheroids resembled accumulation in primary rat hepatocytes cultured on a micro-patterned 3D-collagen gel [16]. Importantly, a pronounced increase in OATP1B3 expression was observed in HepG2 spheroids compared to 2D culture. Inhibition of OATP1B3 by rifampin inhibited CLF accumulation in spheroids, indicating the central role of OATP1B3 in bile acid transport in our system. OATP1B3 plays an important role in hepatic uptake of drugs and various endogenous substrates [39]. Current EMA and FDA guidelines require new chemical entities to be tested for their effects on OATP1B3 (EMA 21 June 2012; FDA Feb 2012) therefore, this HepG2 spheroid model may be suitable for evaluating effects on OATP1B3 activity and bile salt transport.

Induction of CYP450 enzymes is a complex phenomenon mediated by activation of nuclear receptors and gene transcription. It was reported that the low levels of CYP450 enzymes in HepG2 cells is due to the absence of nuclear receptors that regulate their induction [6, 7]. In HepG2 spheroid cultures, the basal levels of nuclear receptors aryl hydrocarbon receptor (AhR), constitutive androstane receptor (CAR) and pregnane X receptor (PXR) were higher compared to monolayer culture. CAR and PXR are regarded as master regulators in drug metabolism [40, 41]. The increased expression of xenobiotic receptors in the spheroid model may make it suitable to study drug-drug interactions mediated by CYP450 enzymes.

Many compounds induce toxicity due to their reactive intermediates [31]. We observed increased functional activity of several important CYP450 enzymes, such as CYP3A4, 2C9 and 2D6 which are involved in metabolism of approximately 80% of marketed drugs [42]. This increased metabolic competence may improve the predictive power of 3D cytotoxic assays. Current in vitro models have limitations for repeated drug exposures studies, which may often be required to accurately reflect drug metabolism in humans. Repeat exposures of HepG2 spheroids resulted in increased sensitivity to DILI compounds compared to a 24 h cytotoxic assessment. Out of 8 hepatotoxic compounds tested, six showed increased sensitivity to repeated drug exposures in 3D cultures. The TC50 of acetaminophen, which is metabolized by CYP2E1 and CYP1A2 was 9.4 mM in 3D repeated exposures, (which is below its 100X Cmax, a scaling factor that represented a reasonable cut-off to differentiate toxic drugs in a study using primary human hepatocytes [17]), whereas for single exposure in 2D cultures, the TC50 was approximately 24 mM. The increased sensitivity with repeated exposures might indicate a mechanistic toxic response over time with DILI compounds. Bosentan, which is metabolized by CYP2C9 and CYP3A4, is known to impair bile acid transport leading to liver toxicity [43]. The TC50 of bosentan in repeat dosing was 400 µM. Although many fold higher than the Cmax (Cmax: 1 µM) no toxicity was observed in 24 h exposures of 2D and 3D cultures. Valproic acid undergoes biotransformation via glucuronidation and CYP2C9, 2A6, 2B6 [44,

45] and liver toxicity is characterized by microvesicular steatosis [46]. The TC50 of valproic acid in 3D repeated exposures was 4 mM, whereas in 2D culture it was ~22 mM. Further development and validation of the 3D spheroid assay may enable its use for prediction of cholestasis and steatosis.

3D spheroids were also sensitive in identifying toxicity induced by the withdrawn drugs, troglitazone and trovafloxacin mesylate. Troglitazone, which is mainly metabolized by CYP3A4, is toxic in our model with a TC50 of 100 µM (15X Cmax). Trovafloxacin mesylate had a TC50 of 5.6 µM, which was close to the human therapeutic Cmax (~4 µM) whereas single exposures were not toxic below 100 µM, demonstrating the significant effect of repeated exposure on sensitivity. Trovafloxacin is primarily metabolized in liver by phase II metabolism (glucuronidation 13.2%, N-acetylation 10.4% and N-sulphoconjugation 4.1% [47]. The increased sensitivity in 3D compared to 2D may be due to the enhanced phase II activity in HepG2 spheroids. Immune mediators, such as TNFα play an important role in sensitization to trovafloxacin-induced hepatotoxicity [48] under conditions of inflammatory stress. Further studies are needed to establish whether the increased sensitivity of HepG2 spheroids involves autocrine signaling by immune mediators or whether the mechanism of toxicity in vitro differs from the mechanism of toxicity *in vivo*. Interestingly, troglitazone was not toxic in HepaRG spheroids [13], whereas toxicity was donor dependent for troglitazone and valproic acid in human primary hepatocytes [18], highlighting the differential sensitivities of different *in vitro* models.

In summary, our findings suggest that the culture of HepG2 cells as spheroids on extracellular matrix-rich hydrogels improves their overall suitability for safety assessment studies. Further validation of this model with a large set of compounds is required to assess its potential use in preclinical safety studies. Development of this model by incorporating co-cultures with other hepatic cells (Kupffer cells, stellate cells) may further improve liver characteristics and prediction of drug toxicity in humans.

REFERENCES

1 MacDonald, J. S. & Robertson, R. T. Toxicity testing in the 21st century: a view from the pharmaceutical industry. Toxicol Sci 110, 40-46, doi:10.1093/toxsci/kfp088 (2009).

2 LeCluyse, E. L. Human hepatocyte culture systems for the in vitro evaluation of cytochrome P450 expression and regulation. European journal of pharmaceutical sciences : official journal of the European Federation for Pharmaceutical Sciences 13, 343-368 (2001).

3 Madan, A. et al. Effects of prototypical microsomal enzyme inducers on cytochrome P450 expression in cultured human hepatocytes. Drug metabolism and disposition: the biological fate of chemicals 31, 421-431 (2003).

4 Guo, L. et al. Similarities and differences in the expression of drug-metabolizing enzymes between human hepatic cell lines and primary human hepatocytes. Drug metabolism and disposition: the biological fate of chemicals 39, 528-538, doi:10.1124/dmd.110.035873 (2011).

5 Wilkening, S., Stahl, F. & Bader, A. Comparison of primary human hepatocytes and hepatoma cell line Hepg2 with regard to their biotransformation properties. Drug metabolism and disposition: the biological fate of chemicals 31, 1035-1042, doi:10.1124/dmd.31.8.1035 (2003).

6 Naspinski, C. et al. Pregnane X receptor protects HepG2 cells from BaP-induced DNA damage. Toxicological sciences : an official journal of the Society of Toxicology 104, 67-73, doi:10.1093/toxsci/kfn058 (2008).

7 Kanno, Y. & Inouye, Y. A consecutive three alanine residue insertion mutant of human CAR: a novel CAR ligand screening system in HepG2 cells. The Journal of toxicological sciences 35, 515-525 (2010).

8 Haouzi, D. et al. Three-dimensional polarization sensitizes hepatocytes to Fas/CD95 apoptotic signalling. Journal of cell science 118, 2763-2773, doi:10.1242/jcs.02403 (2005).

9 LeCluyse, E. L., Witek, R. P., Andersen, M. E. & Powers, M. J. Organotypic liver culture models: meeting current challenges in toxicity testing. Critical reviews in toxicology 42, 501-548, doi:10.3109/10408444.2012.682115 (2012).

10 Zhang, F., Xu, R. & Zhao, M.-j. QSG-7701 human hepatocytes form polarized acini in three-dimensional culture. Journal of cellular biochemistry 110, 1175-1186, doi:10.1002/jcb.22632 (2010).

11 Fey, S. J. & Wrzesinski, K. Determination of drug toxicity using 3D spheroids constructed from an immortal human hepatocyte cell line. Toxicol Sci 127, 403-411, doi:10.1093/toxsci/kfs122 (2012).

12 Nakamura, K. et al. Evaluation of drug toxicity with hepatocytes cultured in a micro-space cell culture system. Journal of bioscience and bioengineering 111, 78-84, doi:10.1016/j.jbiosc.2010.08.008 (2011).

13 Gunness, P. et al. 3D organotypic cultures of human HepaRG cells: a tool for in vitro toxicity studies. Toxicol Sci 133, 67-78, doi:10.1093/toxsci/kft021 (2013).

14 Tostoes, R. M. et al. Human liver cell spheroids in extended perfusion bioreactor culture for repeated-dose drug testing. Hepatology 55, 1227-1236, doi:10.1002/hep.24760 (2012).

15 Godoy, P. et al. Recent advances in 2D and 3D in vitro systems using primary hepatocytes, alternative hepatocyte sources and non-parenchymal liver cells and their use in investigating mechanisms of hepatotoxicity, cell signaling and ADME. Arch Toxicol 87, 1315-1530, doi:10.1007/s00204-013-1078-5 (2013).

16 Matsui, H., Takeuchi, S., Osada, T., Fujii, T. & Sakai, Y. Enhanced bile canaliculi formation enabling direct recovery of biliary metabolites of hepatocytes in 3D collagen gel microcavities. Lab on a chip 12, 1857-1864, doi:10.1039/c2lc40046d (2012).

17 Xu, J. J. et al. Cellular imaging predictions of clinical drug-induced liver injury. Toxicol Sci 105, 97-105, doi:10.1093/toxsci/kfn109 (2008).

18 Khetani, S. R. et al. Use of micropatterned cocultures to detect compounds that cause drug-induced liver injury in humans. Toxicol Sci 132, 107-117, doi:10.1093/toxsci/kfs326 (2013).

19 Asthana, A. & Kisaalita, W. S. Microtissue size and hypoxia in HTS with 3D cultures. Drug Discov Today 17, 810-817, doi:10.1016/j.drudis.2012.03.004 (2012).

20 Hirschhaeuser, F. et al. Multicellular tumor spheroids: an underestimated tool is catching up again. J Biotechnol 148, 3-15, doi:10.1016/j.jbiotec.2010.01.012 (2010).

21 LeCluyse, E. L., Audus, K. L. & Hochman, J. H. Formation of extensive canalicular networks by rat hepatocytes cultured in collagen-sandwich configuration. Am J Physiol 266, C1764-1774

(1994).
22 Bahrami, A., Truong, L. D. & Ro, J. Y. Undifferentiated tumor: true identity by immunohistochemistry. Archives of pathology & laboratory medicine 132, 326-348, doi:10.1043/1543-2165(2008)132[326:UTTIBI]2.0.CO;2 (2008).
23 Wang, L. & Boyer, J. L. The maintenance and generation of membrane polarity in hepatocytes. Hepatology 39, 892-899, doi:10.1002/hep.20039 (2004).
24 Jedlitschky, G., Hoffmann, U. & Kroemer, H. K. Structure and function of the MRP2 (ABCC2) protein and its role in drug disposition. Expert opinion on drug metabolism & toxicology 2, 351-366, doi:10.1517/17425255.2.3.351 (2006).
25 Ng, S. et al. Improved hepatocyte excretory function by immediate presentation of polarity cues. Tissue engineering 12, 2181-2191, doi:10.1089/ten.2006.12.2181 (2006).
26 Kobayashi, Y. et al. Transport mechanism and substrate specificity of human organic anion transporter 2 (hOat2 [SLC22A7]). The Journal of pharmacy and pharmacology 57, 573-578, doi:10.1211/0022357055966 (2005).
27 Sweet, D. H. Organic anion transporter (Slc22a) family members as mediators of toxicity. Toxicol Appl Pharmacol 204, 198-215, doi:10.1016/j.taap.2004.10.016 (2005).
28 Choi, M. H., Skipper, P. L., Wishnok, J. S. & Tannenbaum, S. R. Characterization of testosterone 11 beta-hydroxylation catalyzed by human liver microsomal cytochromes P450. Drug metabolism and disposition: the biological fate of chemicals 33, 714-718, doi:10.1124/dmd.104.003327 (2005).
29 Chen, G. et al. Investigation of testosterone, androstenone, and estradiol metabolism in HepG2 cells and primary culture pig hepatocytes and their effects on 17betaHSD7 gene expression. PLoS One 7, e52255, doi:10.1371/journal.pone.0052255 (2012).
30 Fredriksson, L. et al. Diclofenac inhibits tumor necrosis factor-Œ±-induced nuclear factor-ŒƒB activation causing synergistic hepatocyte apoptosis. Hepatology (Baltimore, Md.) 53, 2027-2041, doi:10.1002/hep.24314 (2011).
31 Guengerich, F. P. Cytochrome P450s and other enzymes in drug metabolism and toxicity. The AAPS journal 8, E101-111, doi:10.1208/aapsj080112 (2006).
32 de Waart, D. R. et al. Hepatic transport mechanisms of cholyl-L-lysyl-fluorescein. J Pharmacol Exp Ther 334, 78-86, doi:10.1124/jpet.110.166991 (2010).
33 Vavricka, S. R., Van Montfoort, J., Ha, H. R., Meier, P. J. & Fattinger, K. Interactions of rifamycin SV and rifampicin with organic anion uptake systems of human liver. Hepatology 36, 164-172, doi:10.1053/jhep.2002.34133 (2002).
34 Abe, K., Bridges, A. S. & Brouwer, K. L. Use of sandwich-cultured human hepatocytes to predict biliary clearance of angiotensin II receptor blockers and HMG-CoA reductase inhibitors. Drug metabolism and disposition: the biological fate of chemicals 37, 447-452, doi:10.1124/dmd.108.023465 (2009).
35 Hoffmaster, K. A. et al. P-glycoprotein expression, localization, and function in sandwich-cultured primary rat and human hepatocytes: relevance to the hepatobiliary disposition of a model opioid peptide. Pharm Res 21, 1294-1302 (2004).
36 Mueller, D., Kramer, L., Hoffmann, E., Klein, S. & Noor, F. 3D organotypic HepaRG cultures as in vitro model for acute and repeated dose toxicity studies. Toxicol In Vitro 28, 104-112, doi:10.1016/j.tiv.2013.06.024 (2014).
37 Kelm, J. M., Timmins, N. E., Brown, C. J., Fussenegger, M. & Nielsen, L. K. Method for generation of homogeneous multicellular tumor spheroids applicable to a wide variety of cell types. Biotechnol Bioeng 83, 173-180, doi:10.1002/bit.10655 (2003).
38 Malinen, M. M., Palokangas, H., Yliperttula, M. & Urtti, A. Peptide Nanofiber Hydrogel Induces Formation of Bile Canaliculi Structures in Three-Dimensional Hepatic Cell Culture. Tissue Eng Part A, doi:10.1089/ten.TEA.2012.0046 (2012).
39 van de Steeg, E., van Esch, A., Wagenaar, E., Kenworthy, K. E. & Schinkel, A. H. Influence of human OATP1B1, OATP1B3, and OATP1A2 on the pharmacokinetics of methotrexate and paclitaxel in humanized transgenic mice. Clinical cancer research : an official journal of the American Association for Cancer Research, doi:10.1158/1078-0432.CCR-12-2080 (2012).
40 Kublbeck, J. et al. New in vitro tools to study human constitutive androstane receptor (CAR) biology: discovery and comparison of human CAR inverse agonists. Mol Pharm 8, 2424-2433, doi:10.1021/mp2003658 (2011).
41 di Masi, A., De Marinis, E., Ascenzi, P. & Marino, M. Nuclear receptors CAR and PXR: Mo-

lecular, functional, and biomedical aspects. Mol Aspects Med 30, 297-343, doi:10.1016/j.mam.2009.04.002 (2009).

42 Wienkers, L. C. & Heath, T. G. Predicting in vivo drug interactions from in vitro drug discovery data. Nat Rev Drug Discov 4, 825-833, doi:10.1038/nrd1851 (2005).

43 Fattinger, K. et al. The endothelin antagonist bosentan inhibits the canalicular bile salt export pump: a potential mechanism for hepatic adverse reactions. Clinical pharmacology and therapeutics 69, 223-231, doi:10.1067/mcp.2001.114667 (2001).

44 Tang, W. & Abbott, F. S. Bioactivation of a toxic metabolite of valproic acid, (E)-2-propyl-2,4-pentadienoic acid, via glucuronidation. LC/MS/MS characterization of the GSH-glucuronide diconjugates. Chemical research in toxicology 9, 517-526, doi:10.1021/tx950120y (1996).

45 Kiang, T. K. et al. Contribution of CYP2C9, CYP2A6, and CYP2B6 to valproic acid metabolism in hepatic microsomes from individuals with the CYP2C9*1/*1 genotype. Toxicol Sci 94, 261-271, doi:10.1093/toxsci/kfl096 (2006).

46 Silva, M. F. et al. Valproic acid metabolism and its effects on mitochondrial fatty acid oxidation: a review. Journal of inherited metabolic disease 31, 205-216, doi:10.1007/s10545-008-0841-x (2008).

47 Vincent, J., Teng, R., Dalvie, D. K. & Friedman, H. L. Pharmacokinetics and metabolism of single oral doses of trovafloxacin. American journal of surgery 176, 8S-13S (1998).

48 Beggs, K. M., Fullerton, A. M., Miyakawa, K., Ganey, P. E. & Roth, R. A. Molecular Mechanisms of Hepatocellular Apoptosis Induced by Trovafloxacin-Tumor Necrosis Factor-alpha Interaction. Toxicol Sci 137, 91-101, doi:10.1093/toxsci/kft226 (2014).

49 Guideline on the investigation of drug interactions. European Medicines Agency, 2012 June 21, Available at: http://www.ema.europa.eu/docs/en_GB/document_library/Scientific_guideline/2012/07/WC500129606.pdf) Accessed: 31 Jan 2014.

50 FDA guidance for drug interactions- study design, data analysis, implications for dosing and labeling recommendations, CDER, 2012 Feb. Available at: http://www.fda.gov/downloads/Drugs/GuidanceComplianceRegulatoryInformation/Guidances/ucm292362.pdf Accessed: 31 Jan 2014.

SUPPLEMENTARY DATA

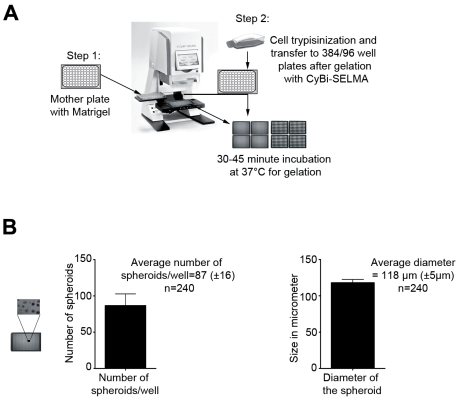

Supplementary S1. *Schematic representation of 3D HepG2 spheroid culture*. (A) Matrigel was added to the plates using the Cybi-Selma semiautomatic pipettor. A 96-well mother plate was prepared by manually pipetting Matrigel into the wells. Plates were then incubated for 30-45 min at 37°C for gelation before adding the required number of cells. (B) Number and area of spheroids after 28-days in 3D cell cultures.

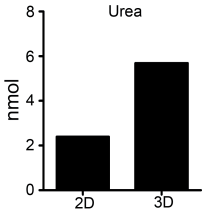

Supplementary S2. *Urea production in 2D and 3D HepG2 cells*. Data normalized to 6X104 cells. Data is representative of 2 independent experiments.

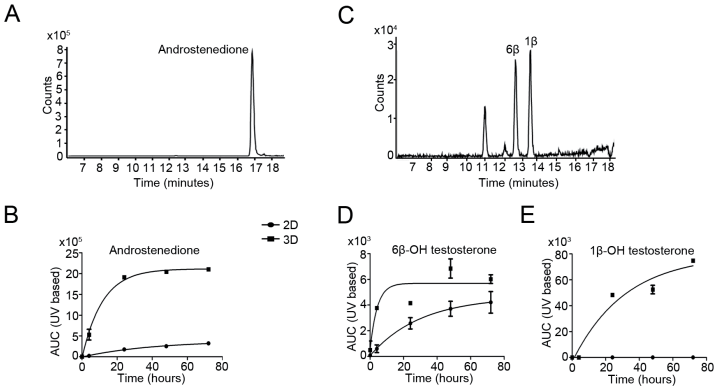

Supplementary S5. *Biotransformation of testosterone in 2D and 3D HepG2 cultures*. Extracted ion chromatogram of androstenedione (m/z 287,20) in a 72hr 3D sample (A). Time curves of androstenedione formation after exposure of 2D/3D cell cultures (B). Data is representative of two independent experiments. Extracted ion chromatogram of hydroxylated testosterone (m/z 305, 19) in a 72hr 3D sample (C), Time curves of 1-β and 6β-hydroxy testosterone formation (D and E) after exposure. Quantification is based on UV, and corrected for background. Data is representative of two independent experiments.

Gene	Forward primer	Reverse primer
GAPDH	AGCCACATCGCTCAGACACC	ACCCGTTGACTCCGACCTT
CYP3A4[1]	CAGGAGGAAATTGATGCAGTTTT	GTCAAGATACTCCATCTGTAGCACAGT
CYP1A2	GCCTTCATCCTGGAGACCTT	AGCGTTGTGTCCCTTGTTG
CYP2E1	TTCAGCGGTTCATCACCCT	GAGGTATCCTCTGAAAATGGTGTC
CYP2C9[2]	ACATCAGCAAATCCTTAACCAATCT	GGGTTTCAGGCCAAAATACAGA
CYP2C19	GTCCAGAGATACATCGACCTCA	AGTGAGGGAAGTTAATATGGTTGTG
CYP4F3	CATCAAGCCTGTGCTCTTTG	CTTTTCACCAGCACTCAGCA
CYP2D6[2]	CGCATCCCTAAGGGAACGA	TTCCAGACGGCCTCATCCT
UGT1A1[3]	AACTTTCTGTGCGACGTGGTT	GTCACCTCTCTCTGAAGGAATTCTG
UGT1A6[3]	AGCCCAGACCCTGTGTCCTA	CCACTCGTTGGGAAAAAGTCA
UGT2A3	GGTCACTGTTTCAAAATGTTACAGAA	TTCCTTTGTACCTCCATAACACC
UGT2B4	CCAAATGTTGAGTTCGTTGG	GCTCTGGACAAACTCTTCCATT
SULT2A1	TGAGAGAGGAGAAAAACTT	TCTTTCCCAGGAATTGAC
OAT2	TAGCTGTCACCCTGCCTTGT	CATGGCCTTGGGTCAGAA
OAT7	GCATCCTAGGCGGTCATTTA	TGGCAACCTGGAGGTAACAC
AHR	CAACATCACCTACGCCAGTC	GCTTGGAAGGATTTGACTTGA
CAR	CAGGTGACATGCTGCCTAAG	TCAGCTCATCTTCCCTACTGG
PXR	GGACGCTCAGATGAAAACCT	AACTCGCAGCCACTGCTAAG
Ki67	CCAAAAGAAAGTCTCTGGT	CCTGATGGTTGAGGCTGTTC

Supplementary S3. Primer sequences used for real-time PCR analysis.

[1] Kikuchi R, McCown M, Olson P, Tateno C, Morikawa Y, Katoh Y, et al. Effect of hepatitis C virus infection on the mRNA expression of drug transporters and cytochrome p450 enzymes in chimeric mice with humanized liver. Drug metabolism and disposition: the biological fate of chemicals 2010;38:1954-1961.
[2] Westerink WMa, Schoonen WGEJ. Cytochrome P450 enzyme levels in HepG2 cells and cryopreserved primary human hepatocytes and their induction in HepG2 cells. Toxicology *in vitro* : an international journal published in association with BIBRA 2007;21:1581-1591.
[3] Westerink WM, Schoonen WG. Phase II enzyme levels in HepG2 cells and cryopreserved primary human hepatocytes and their induction in HepG2 cells. Toxicol *In Vitro* 2007;21:1592-1602.

Supplementary S4. Protocol used to analyse phase I metabolites at Pharmacelsus GmBH.

Compound exposure:

Substrate mix was exposed to 2D and 3D cells in 96-well plates. Spheroids stop proliferating after day 14 and they have equal cell number between 21-day and 28-days as determined using ATPlite assay. Same amount of cells (20x103 cells/well) were seeded to 2D plates and after 24 hours substrate mix was added to the cells and samples were collected at 0, 4, 24 and 48 h from a pool of 8 wells of 96-well plate at each time point and the data indicates nmol of metabolite formed/ 1.6x105 cells initial cell density. Samples were stored at -80 degrees and shipped on dry ice to Pharmacelsus GmBH for further analysis as explained below.

Sample preparation:

Cell culture supernatants were precipitated with the twofold volume of acetonitrile supplemented with the internal standard (1 μM griseofulvin), vigorously shaken (10

min) and centrifuged (5,000xg).

LC-MS conditions:

The HPLC system consisted of U-HPLC pump and an auto sampler (both by Thermo Fisher Scientific, Dreieich, Germany). Mass spectrometry was performed on a Q-Exactive mass spectrometer (Orbitrap technology, Thermo Fisher Scientific) equipped with a heated electrospray interface (Thermo Fisher Scientific) and connected to a PC running the standard software Xcalibur 2.2. The HPLC pump flow rate was set to 600 μl/min and the compounds were separated on a Gemini C6-phenyl 3 μm, 50x2.0 mm analytical column (Phenomenex, Aschaffenburg, Germany) with corresponding precolumn. Analytes were separated by gradient elution with acetonitrile as organic phase (A) and 10 mM ammonium acetate as aqueous phase (B) (% A (t (min), 0(0-0.1)-97(0.4-1.7)-0(1.8–3.0). The mass resolution of the Orbitrap was set to 17,500. Further analyser settings were as follows: max. trap injection time 120 ms, sheath gas 40, aux gas 10, sweep gas 2, capillary voltage 4 kV, capillary temperature 350°C, H-ESI heater temperature 350°C. Full MS selected ion monitoring (SIM) analysis was applied using fast scan-to-scan polarity switching to analyse all metabolites in a single sample run. Target ions for SIM analysis ([M+H]+ or [M-H]-, respectively) were m/z 278.1751 (1-hydroxybufuralol), m/z 342.0804 (1'-hydroxymidazolam) and m/z 353.0786 (griseofulvin, internal standard) in the positive mode and m/z 183.9796 (6-hydroxychlorzoxazone) and m/z 310.0033 (4'-hydroxydiclofenac) in the negative mode. Retention times were 1.07 min (1-hydroxybufuralol), 1.20 min (1'-hydroxymidazolam), 1.10 min (6-hydroxychlorzoxazone), 1.13 min (4'-hydroxydiclofenac) and 1.23 min (griseofulvin).

Calibration standards and quantification:

The stock solutions of each metabolite were prepared in acetonitrile/water (1:1, v/v), except for 6-hydroxychlorzoxazone was prepared in acetonitrile and methanol, respectively. A cocktail working solution was prepared containing all metabolites at a concentration of 250 μM. Calibration samples were generated in cell culture medium to achieve the final concentrations of 5000, 2400, 1200, 400, 100, 25, 6.25, 2.08, 1.04, and 0.52 nM for each metabolite. Calibration curves for each metabolite were represented by the plots of the peak-area ratio (metabolite/internal standard) versus the nominal concentration of the metabolite in cell culture medium. The line of best fit was generated using quadratic regression and weighing as appropriate. Metabolite concentrations in experimental samples were calculated from the resulting area ratio and the regression equation of the calibration curve.

Supplementary S6. Protocol used to analyze testosterone metabolism and phase II metabolism (Glucuronidation and sulphation).

Qualitative and quantitative analysis of phase I (Testosterone) and Phase II (Diclofenac glucuronidation and Paracetamol Sulfation).

The total number of cells/well in 3D cell culture was measured by ATP-lite assay and an equal number of cells were seeded in 2D culture. 2D and 3D HepG2 cells were incubated with testosterone (500 µM), paracetamol (1mM) and diclofenac (500 µM). Incubations were terminated at 0, 4, 24, 48 and 72 hours by adding perchloric acid (1% v/v) final concentration in case of testosterone, perchloric acid (1%V/V) in 50% v/v acetonitrile for paracetamol and ice cold methanol (50% v/v) for diclofenac.

The samples were centrifuged at 14,000 rpm for 15 minutes. Supernatants were stored at -80°C until analysis. The analytical method used for diclofenac was described previously (1). For paracetamol the same method was used, with the only difference using of a Luna C18 reversed-phase column (150 mm x 4.6mm, 5 µm i.d.) (Phenomenex, Torrance, CA). For testosterone the analysis of metabolites was done using a Shimadzu Prominence HPLC system equipped with a Luna C18 reversed-phase column (150 mm x 4.6mm, 5 µm i.d.) (Phenomenex, Torrance, CA) and a SPD-2A UV/VIS detector (Shimadzu, Kyoto, Japan). The mobile phase for both HPLC and LC-MS/MS analysis (flow rate 0.5 mL/min) consisted of a gradient constructed of 0.1% formic acid in water (solution A) and 0.1% formic acid in methanol (solution B). Testosterone and its metabolites were eluted using an isocratic elution at 50% B for 1 min after sample loading, followed by a linear gradient from 50 to 99% B from 1 to 19 minutes. The final gradient composition was maintained for 1 minute, after which the column was re-equilibrated with the initial gradient composition. Metabolites were quantified by integration of analytes detected at 254 nm. Retention times of analytes were: 6β-hydroxy testosterone at 12.8 min, 1β-hydroxy testosterone at 13.5 min, androstenedione at 16.8 min, testosterone at 18 min.

To identify metabolites by LC-MS, the final time points were pooled and extracted with 3 volumes of dichloromethane. The combined fractions were evaporated to dryness under a stream of nitrogen and reconstituted in 200µL 50% methanol. An Agilent 1200 Series Rapid resolution LC system was connected to a hybrid quadrupole-time-of-flight (Q-TOF) Agilent 6520 mass spectrometer (Agilent Technologies, Waldbronn, Germany), equipped with an electrospray ionization (ESI) source operating in the positive mode. The MS ion source parameters were set with a capillary voltage of 3500 V; nitrogen was used as the desolvation (12L/min) and nebulizing gas (pressure 60 psig) at a constant gas temperature of 350°C. Nitrogen was used as a collision gas with collision energy of 25 V. MS spectra were acquired using automated full scan MS/MS analysis over m/z range of 50–1000 using a scan rate of 1.003 spectra/s. Metabolite identification was established by comparison with refer-

ence compounds. Androstenedione was obtained from Sigma Aldrich (Zwijndrecht, the Netherlands). Hydroxy metabolites of testosterone were identified by comparison with metabolites formed by recombinant CYP3A4 (2).

1. Dragovic S. Boerma JS, Vermeulen NP, Commandeur JN Effect of human glutathione S-transferases on glutathione-dependent inactivation of cytochrome P450-dependent reactive intermediates of diclofenac .Chem Res Toxicol 2013;26:1632-41
2. Krauser JA, Voehler M, Tseng LH, Schefer AB, Godejohann M, Guengerich FP. Testosterone 1 beta-hydroxylation by human cytochrome P450 3A4. Eur J Biochem 2004;271:3962-3969.

Supplementary S7. List of compounds used for toxicity assessment.

	Compound	Solvent	cMax (µM)	100XCmax (µM)	Concentration range tested (µM)	TC50 (µM)
1	Aspirin	DMSO	5.526	552.6	4.64 to 1000	N/A
2	Dexamethasone	DMSO	0.224	22.4	2.15 to 464	N/A
3	Fluoxetine	DMSO	0.049	4.9	0.0215 to 4.64	N/A
4	Dextromethorphan HBr	DMSO	0.028	2.8	0.010 to 2.15	N/A
5	Isoniazid	Culture media	76.6	7660	464 to 100000	~14000
6	Troglitazone	DMSO	6.387	638.7	1 to 215	~100
7	Acetaminophen	Culture media	139	13900	464 to 100000	~9400
8	Nimesulide	DMSO	6.5	650	10 to 2150	~1000
9	Bosentan	DMSO	1	100	4.64 to 1000	~400
10	Trovafloxacin mesylate	DMSO	4.078	407.8	1 to 215	~5.6
11	Diclofenac	DMSO	8.023	802.3	10 to 2150	~530
12	Valproic acid	Culture media	30.086	3008.6	464 to 100000	~4000